The Journal of Energy: Engineering & Management
Vol. 12, No. 4, Winter 2023, P. 30-43
Research Article

A New Type-II Fuzzy Logic Control-Based Energy Management Strategy for Improving Fuel Cell Durability and Fuel Economy of Hybrid Electric Vehicle

Majid Keshavarz[1], Nooshin Bigdeli[2], Aref Shahmansoorian[3*]

[1] Faculty of Engineering, Imam Khomeini International University,Qazvin, Iran
majidkeshavarz2392@gmail.com
[2] Faculty of Engineering, Imam Khomeini International University, Qazvin, Iran
n.bigdeli@eng.ikiu.ac.ir
[3] Faculty of Engineering, Imam Khomeini International University, Qazvin, Iran
shahmansoorian@eng.ikiu.ac.ir

Accepted: 8/11/2022 **Received:** 29/01/2023

Abstract
This paper presents a novel energy management strategy (EMS) for the hybrid electric vehicle with fuel cell/battery/ultra-capacitor energy sources (FCHEV). For improving the durability and fuel economy of the fuel cell system in FCHEV, the proposed EMS utilized a close-loop control strategy that combines fuzzy logic control (FLC) and a frequency decoupling-based model based on an adaptive low-pass filter and wavelet transform methods. Uncertainty as a powerful tool is utilized to design flexible strategies using type-II FLC based on the charge state of power storage systems. Furthermore, the designed frequency decoupling-based control system separates three optimal frequency components of the required power to supply it by fuel cell, battery, and ultra-capacitor systems based on their individual characteristics and limitation of the power fluctuation on the fuel cell system. Finally, a dynamic performance test used the ADVISOR simulator under the World Light Vehicle Test Cycle (WLTC) to compare the proposed strategy with different strategies. According to the simulation results, the proposed strategy ensures the safety of the ultra-capacitor and battery park and improves the durability of the fuel cell while reducing the hydrogen consumption maximum by 14.6% in comparison with different strategies under similar driving conditions.

Keywords: hybrid electric vehicle, energy management strategy, adaptive control methods, type-II fuzzy logic control, fuel economy.

* Corresponding author
doi: 10.22052/JEEM.2023.113684

1. Introduction

Fuel Cell/Battery/Ultra-capacitor Hybrid Electric Vehicle has more pollution reduction as well as more health and environmental benefits than internal combustion engine vehicles. Furthermore, FCHEVs have a great capacity to present a valid solution for the limitation of other electric vehicles. However, the main impact of the energy management system in FCHEVs is the capability of the power supply which is based on the individual characteristics of every power supply [1, 2].

Recently, many researchers have presented various EMS with different approaches for FCHEVs. All of the presented EMSs can be classified into three main categories: Rule-based, optimization-based, and learning-based strategies.

Rule-based strategies, as a suitable control method for real-time operation/implementation, are affected more by driving conditions because of the simple-rule base design. Therefore, as reviewed in Table 1, many researchers presented several types of rule-based control methods with different operations along their advantages and disadvantages [3], which were related to optimization and adaptivity problems [4]. Furthermore, optimization-based and learning-based strategies have been reported in Table 1 as two main different EMS methods for hybrid electric vehicles [5, 6].

Because of the independence of the mathematical technique, fuzzy control was provided as an efficient and accurate strategy to cope with nonlinear challenges in constructing a valid control method for the FCHEV energy system [7]. Besides, so many researchers have combined fuzzy control with other control methods, which depended on a plenty of engineering experiences. In [8], an adaptive fuzzy control approach was presented for fuel cell/battery hybrid electric vehicles. This approach was modified to obtain smoother and more effective fuel cell power.

To keep flexibility and resistance to uncertainty for incorrect input data, the type-II fuzzy control system

Table 1: Classification of different EMSs for electric vehicles

Rule-based strategies		• Fuzzy control strategy • State machine control strategy • Classical PI control strategy • Frequency decoupling and fuzzy logic strategy (FDFL) • Power prediction
Optimization-based strategies	Global optimization	• Linear programming (LP) • Dynamic programming (DP) • Global extremum seeking (GES) • Genetic algorithm (GA)
	Real-time optimization	• Pontryagin's minimum principle (PMP) • Quadratic programming (QP) • Multi-agent system (MAS) • Stochastic dynamic programming (SDP) • Convex programming • Multi-mode predictive (Markov driving pattern recognizer) • Soft-run strategy • Fractional order extremum seeking method • Dynamic particle swarm optimization
Learning-based strategies		• Reinforcement learning • Supervised learning • Unsupervised learning • Neural network • Multi-mode strategy – learning vector quantization (LVQ)

It demonstrated a powerful and simple design for real-time energy management applications [9]. Recent researchers have developed various fuzzy control-based EMS to increase the resilience of the control system and to enhance significantly fuel efficiency, dynamic properties, and the uncertainty of fuel cell hybrid power systems [10, 11]. However, fuzzy logic control primarily depends on expert knowledge and cannot dynamically react to changes in the vehicle's external environment. In the literature [12], replenishment of the battery was accomplished using a technique which was based on minute variable fuzzy control, and the power distribution between the fuel cell and the battery was further adjusted using the bifurcation approach [13]. Also, a fuzzy-based adaptive controller was created to smooth out the fuel cell output energy [14], and a genetic algorithm (GA) was utilized to fine-tune the settings of the controller to enhance the hybrid system's dynamic properties [15,16]. The majority of the literature mentioned above attempted to improve the FCHEVs' economics; however, there is a lack of research on the endurance of fuel cells.

Fuel cell durability has slowly begun to be included in energy management as a result of the fact that the single factor of FCHEV economics is no longer adequate to fulfill practical demands. Along with increasing hydrogen consumption, a combined control method based on FLC-

FIR filtering can assist to enhance the durability of fuel cells [15].

In this paper, a novel EMS with an adaptive low-pass filter and wavelet transform based on type-II fuzzy control systems is presented. The main contribution is utilizing type-II fuzzy control methods and experimental information to design a flexible and stable EMS for different driving conditions. Therefore, type-II fuzzy control is employed because it has a better performance than conventional fuzzy control in addressing uncertainty. Hence, type-II fuzzy sets are dependent on different experiences by the combination of knowledge collected from experts. The proposed EMS which is based on the frequency decomposition method has never applied a delay in the system response to damage the stability of the system and to decrease its reliability [17]. However, the proposed EMS, based on wavelet transform allowing natural frequency splitting, is well adapted to this strategy specification [18]. The frequency of decoupling-based approach allows for an analysis of the power signal at different scales, which is a suitable method in the hybrid energy source systems.

The proposed EMS deployes the difference between the vehicle's required power and the lower limit of the fuel cell efficiency zone and state of charge (SOC) of the power storage systems as input data to design the fuzzy controller and to solve the output power proportionality coefficient. A low-pass filtering technique is utilized to prevent high fluctuations on fuel cell power while a switching control strategy is included to balance fuel cell's durability with the vehicle's efficiency. This method also ensures that the SOC is maintained within a tolerable range.

Finally, a simulation model is established through Advisor and Matlab2019a/Simulink, and the simulation verification is carried out under the compound driving cycle.

In following comes a list of some contributions and innovations of this study:

- Creating a novel close-loop control model based on type-II fuzzy logic control with an adaptive low-pass filter and wavelet transform.
- Verifying the proposed EMS against the valid compound-driving cycle for the different driving conditions.
- Investigating the optimal power distribution considering the individual properties of each power supply to reach an optimal and stable power distribution.
- Considering the ways whereby the uncertainty of SOC in the power storage system can be stabilized by type-II fuzzy control.
- Improving the durability of fuel cells by reductions in power fluctuations.
- Improving the proposed EMS's dynamic performance parameters based on the ADVISOR simulator.

This paper is organized as follows: In section two, mechanical and electrical models of FCHEV and fuel cell/battery/ultracapacitor are presented. In section three, the structure of the proposed EMS is defined in detail, and the simulation result is evaluated by section four. Finally, section five presents a conclusion to the proposed EMS as well as an elaboration on advantages/disadvantages.

2. Modeling of FCHEV

In this study, the FCHEV structure consists of fuel cell/battery/ultracapacitor energy systems (as illustrated in Fig. 1). The proposed FCHEV employed a battery/ultracapacitor hybrid energy storage system to supply the required power for supporting the fuel cell. The ultra-capacitor and fuel cell systems are connected to the DC bus by a bidirectional and a unidirectional DC/DC converter respectively. The battery system is directly connected to the DC bus to determine and maintain the nominal DC bus voltage.

2.1. Modeling of Vehicle

In this paper, the proposed EMS primarily solves the problem of power distribution, and the required power of the vehicle is distributed to three different power supplies to fulfill the optimal performance challenge of the vehicle. The hybrid energy system approach establishes an FCHEV model to obtain the required power based on the vehicle speed v. Hence, the traction force F_t is determined based on the vehicle speed v, which can be obtained as follows [19]:

$$\begin{cases} F_t = F_i + F_j + F_f + F_w \\ F_i = mg\sin\alpha \\ F_j = \delta m\dfrac{dv}{dt} \\ F_f = f_r mg\cos\alpha \\ F_w = 0.5C_d A\rho v^2 \end{cases} \tag{1}$$

where the friction force (resistance with the road surface), aerodynamic drag force, and required acceleration force are defined as F_f, F_w, and F_j, respectively. Furthermore, the gravity force for driving on non-horizontal roads with a road angle α is considered as F_i. Thus, the defined FCHEV parameters are listed in Table 2. Finally, the required power P_{req} can be determined as a conditional function of the traction force and vehicle speed v, whichare described by the following equation:

$$\begin{cases} P_{req} = F_t \cdot v / \eta_m ,F_t > 0 \\ P_{req} = F_t \cdot v \cdot \eta_m \ ,F_t < 0 \end{cases} \tag{2}$$

where η_m is the efficiency constant of the electric motor.

2.2. Modeling of the Fuel Cell

The main power supply in FCHEV is provided by the fuel cell system, where the fuel cell is transforming chemical energy into electrical power (from the chemical reactions between hydrogen and oxygen). In this study, the global efficiency η_{fc} is considered the fuel cell efficiency coefficient by the following equation [20]:

$$\eta_{fc} = \frac{P_{fc}}{P_{H_2}} \tag{3}$$

where P_{fc} is the fuel cell system supplied power, and ρ_{H_2} is the expected supplied power with hydrogen consumption.

To achieve the optimal global efficiencyη_{fc}, as indicated in Fig. 2, the high-efficiency region of the fuel cell system can be selected in the 2.5kW to 18kW range. Thereafter, FCHEV can reduce hydrogen use to improve fuel economy.

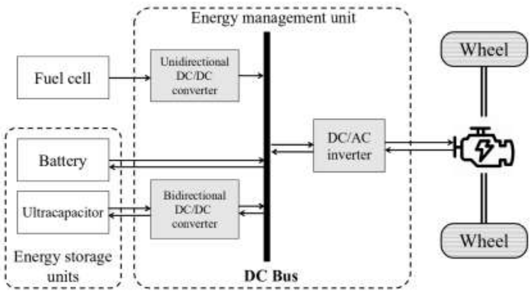

Fig. 1: Fuel cell/battery/ultracapacitor hybrid electric vehicle structure

Table 2: Parameters of the defined FCHEV model

Parameter	Symbol	Value
Vehicle mass	m (kg)	1113
Gravity constant	g (m/s^2)	9.8
Rolling resistance coefficient	f_r	0.6
Aerodynamic drag coefficient	C_d	0.3
Vehicle frontal area	A (m^2)	1.75
Air density	ρ (kg/m^3)	1.22
Conversion coefficient of vehicle rotating mass	δ	1.3

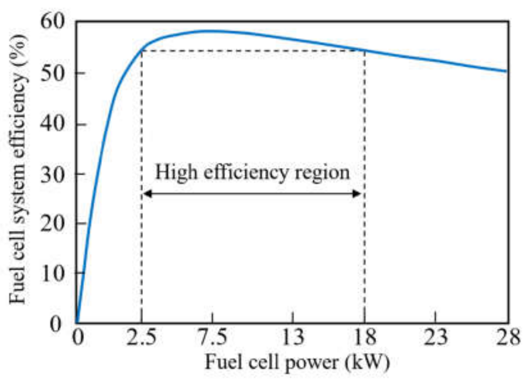

Fig. 2: Fuel cell system's efficiency versus fuel cell's power curve

2.3. Modeling of the Battery

According to the equivalent circuit model, the battery system is defined as a voltage source and equivalent resistance for output characteristics analysis (as shown in Fig. 3(a)).

A suitable range for the battery SOC is a crucial parameter of EMS to prevent overcharge and over-discharge events during different driving conditions. Therefore, the output voltage and SOC of the battery system can be defined as follows [21]:

$$V_b(t) = E_b(t) - R_b i_b(t) \tag{4}$$

$$SOC_b(t) = SOC_b(1) - \eta_b \int \frac{i_b(t)}{3600 Q_b} dt \tag{5}$$

where V_b, E_b, R_b, and i_b are the battery system parameters as output voltage, open voltage, internal resistance, and current respectively. In addition, the battery SOC (SOC_b) with initial SOC ($SOC_b(1)$) is considered, while η_b is charge and discharge efficiency, and Q_b is the nominal capacity.

2.4. Modeling of Ultra-capacitor

The ultra-capacitor system is modeled like an equivalent resistance and capacitor as illustrated in Fig. 3(b). The equivalent capacitor refers to the performance of the discharge and charge states, and the equivalent resistance denotes the ohmic losses of the ultra-capacitor system. FCHEV has to supply/store a large amount of energy in an accelerating/braking state. Hence, the ultra-capacitor system should have sufficient capacity to recycle generated power in the braking state. Furthermore, the ultra-capacitor SOC should be at a reliable charge level to operate optimally in the accelerating state. Therefore, the ultra-capacitor voltage and SOC can be obtained as follows [22]:

$$V_u(t) = E_u(t) - R_c i_c(t) \tag{6}$$

$$SOC_u(t) = \frac{(E_u(t) - 2R_c i_c(t))^2}{V^2_{uc,\max}} \tag{7}$$

where V_b, E_u, i_c, and R_c are terminal voltage, capacitor voltage, load current, and equivalent resistance respectively. Moreover, the ultra-capacitor SOC (SOC_u) is limited to ultra-capacitor's maximum voltage $V_{uc,max}$.

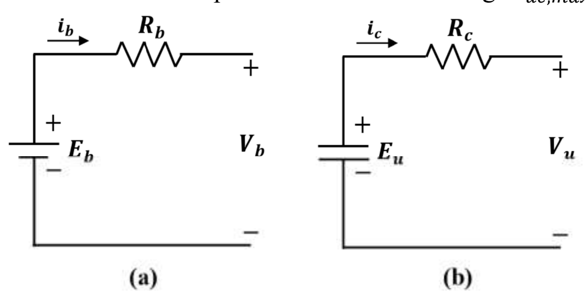

Fig. 3: The equivalent circuits of (a) battery, (b) and ultra-capacitor systems

3. The Proposed EMS for FCHEV

The flowchart of the optimal power distribution process based on the proposed EMS is illustrated in Fig. 4, practically. The proposed EMS consists of three main parts based on the individual characteristics of each power supply as shown in Fig. 5. Three main parts of the proposed EMS are as follows:

- Adaptive low-pass filter based on type-II fuzzy control
- Signal processing unit based on the Haar-wavelet transform
- Power sharing algorithm based on type-II fuzzy control

In the first part, a type-II fuzzy control based on the required power and ultra-capacitor SOC adapted a low-pass filter to decompose high and low-frequency components of the required power. In the next part, the signal processing unit based on the Haar wavelet transform is applied to low-frequency component of the required power. Finally, the output transformed power devoted to the fuel cell and battery systems by another type-II fuzzy control.

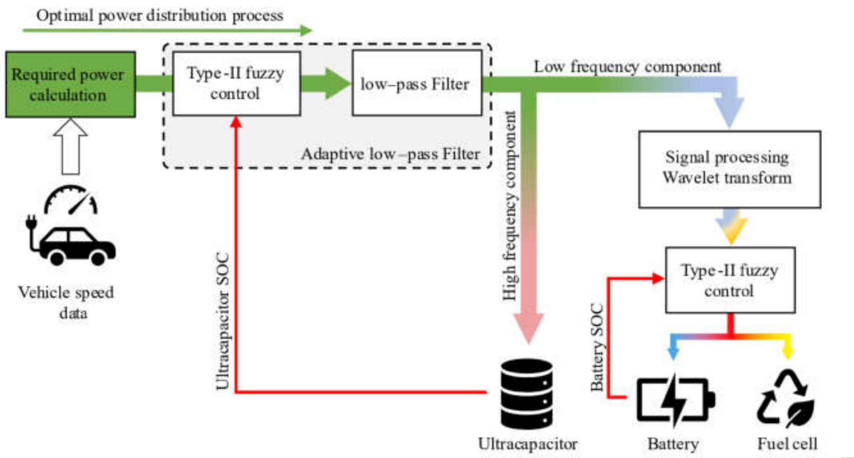

Fig. 4: The flowchart of the proposed EMS process for the optimal power distribution

3.1. Adaptive Low-Pass Filter Based on Type-II Fuzzy Control

In the first part of the proposed EMS, the high-frequency components of the required power are separated by an adaptive low-pass filter effectively. In real-time computation, the proposed adaptive filter which is based on fuzzy control has advantages in computation complexity and design challenges. Hence, the low-pass filter is defined as follows:

$$\begin{cases} G(s) = \dfrac{1}{Ts+1} \\ f_s = \dfrac{1}{T} \end{cases} \tag{8}$$

where $G(s)$ is the transfer function of the low-pass filter with the time constant T, and f_s is the regulating frequency.

To maintain ultra-capacitor SOC in a tolerable range, the ultra-capacitor reference SOC parameter is defined as a function of vehicle speed and ultra-capacitor SOC (as shown in Fig. 5(a)). Therefore, ultra-capacitor reference SOC (SOC_u^{ref}) can be defined as follows:

$$SOC_u^{ref} = \frac{(v_{\max} - v)}{v_{\max}} SOC_u^{\max} \tag{9}$$

where $v_{\max}$ is the maximum speed of FCHEV, and $SOC_u^{\max}$ is the maximum ultra-capacitor SOC.

Consequently, an adjusting frequency increment Δf_s is determined to modify f_s and to guarantee that SOC_u is close to SOC_u^{ref} and changes as a function of driving conditions. Ultimately, the final regulating frequency is given by Eq. (10) as follows:

$$\begin{cases} f_s = f_s^{ref} + \Delta f_s \\ \Delta f_s = k(SOC_u - SOC_u^{ref}) \end{cases} \tag{10}$$

where regulatory factor is defined as k.

To modify low-pass filtering, the designed type-II fuzzy control (FC#1) adapts the time constant in real-time. The primary purpose of FC#1 is to retain the ultra-capacitor SOC in the stable and tolerable range ($0.4 < SOC_u < 1$). Therefore, the ultra-capacitor system would be able to supply/absorb the high-frequency components of the required power in the short-time acceleration or braking state. Consequently, the ultra-capacitor system modifies pressure on fuel cell and battery systems by reductions in their power fluctuations simultaneously. The inputs (the ultra-capacitor SOC and the required power) and the output (regulating frequency) variables of FC#1 as the triangle membership function are illustrated in Fig. 6.

In real-time systems, type-II fuzzy control lets the EMSs utilize the knowledge based on the uncertainty of the different experts (for example, the survey using linguistic labels). Hence, the methodology to design type-II fuzzy controllers from the uncertainty knowledge is presented by [23].

The numerical value of the uncertainty can be defined as a function of the mean and standard deviation criteria for each linguistic label [23]. Additionally, the state of charge quantity in each storage system is a collection of measurement data with mean and standard deviation values. The continual charge/discharge processing during the electric vehicle's lifecycle will decrease the efficiency of the storage system. Hence, as a knowledge-based control approach, the uncertainty on SOC of the power storage systems is a reasonable concept.

In the proposed EMS, the designed type-II fuzzy controllers have a certain uncertainty on battery and ultra-capacitor SOC based on the proposed survey method in [24]. As illustrated in Fig. 6, the uncertainty on ultra-capacitor SOC is considered an uncertain membership function. Because of reductions in the performance efficiency in the lifecycle of FCHEV, the SOC of the storage systems will be measured lower than the actual SOC value.

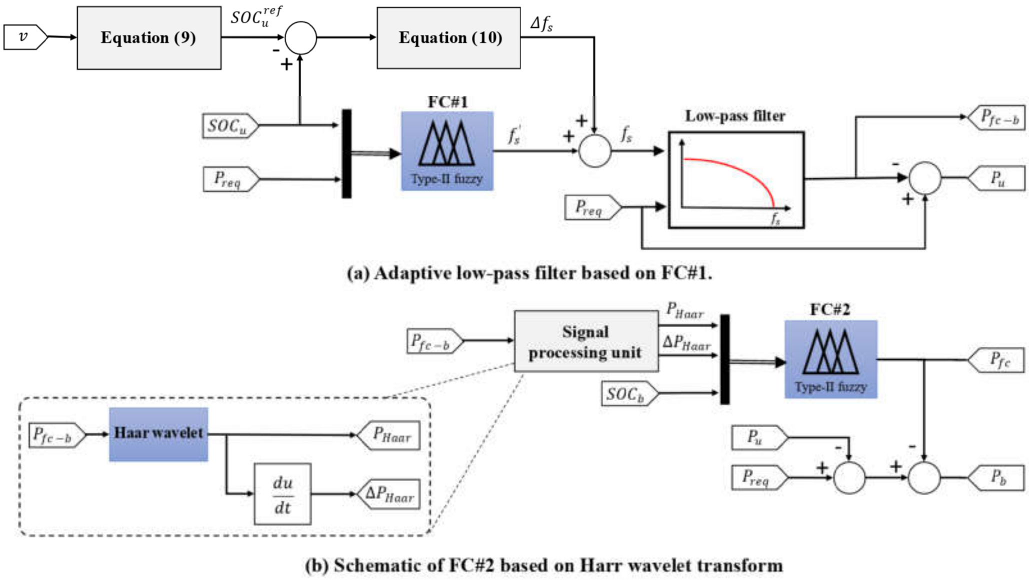

Fig. 5: The proposed EMS schematic

Therefore, the uncertainty on battery and ultra-capacitor SOC is defined as an uncertain membership function to lower values. Finally, the output uncertainty will be considered an internal triangle membership function.

Based on FC#1 rule bases in Fig. 6, when P_{req} is positive big (acceleration state), and ultra-capacitor SOC is big, the f_s will be decreased to provide enormous power. Furthermore, when P_{req} is negative big (braking state) and ultra-capacitor SOC is small, the f_s will be increased to absorb regenerative power by the ultra-capacitor system. For the small P_{req}, the ultra-capacitor only supplies a low level of power to shirk power fluctuations on the fuel cell and battery systems. In addition to avoiding over-discharging/charging of ultracapacitor system, FC#1 should modify f_s with increasing or decreasing ultrcapacitor SOC.

Moreover, when FCHEV runs at low speed in actual driving cycle, acceleration state is likely to happen; therefore, ultra-capacitor SOC should be at a high level to supply the required power. Meanwhile, when FCHEV runs at high speed, braking has a greater probability at the next state. Hence, ultra-capacitor SOC should have sufficient capacity to absorb regenerated power.

3.2. Signal Processing Unit Based on Haar Wavelet Transform

In above contents, the adaptive low-pass filter distributes the high-frequency component of P_{req} to the ultra-capacitor system. The output signal of the low-pass filterP_{fc-b} still includes some high-frequency parts, which cannot directly be supplied by the fuel cell to prevent high fluctuations and durability challenges. Therefore, the proposed EMS presents a pre-processing operation to adjust high-frequency components and signal sharpness of P_{fc-b}.

In this paper, the high and low-frequency components of P_{fc-b} are separated by a wavelet transform; also, the differential of the transformed power has made a valid variable to solve the signal sharpness challenge. In urban driving cycles, especially when the vehicle is accelerating or braking rapidly, there are sharp fluctuations in the required power

According to the one-dimension discrete signal ofP_{fc-b}, this paper utilizes discrete and inverse discrete wavelet transform as follows:

$$W(\lambda,u)=\int s(t)\frac{1}{\sqrt{\lambda}}\Psi(\frac{t-u}{\lambda})dt, \quad (11)$$

$$\lambda=2^j, u=k2^j$$

$$s(t)=\sum_{j=Z}\sum_{k=Z}W(j,k)\Psi_{(j,k)}(t) \quad (12)$$

where $s(t)$, λ, and u are the original signal, the scale parameter, and the position parameter respectively. Also, ψ is defined as a mother wavelet transform function with wavelet coefficient$W$.

In this study, the proposed EMS can regard the power distribution as one stationary process instantly [25]. The Haar wavelet in the time domain has a shorter filter length advantage than other transform models. To fulfill the trade-off between different performance objectives, the proposed EMS chooses the Haar wavelet as the mother wavelet transform to simplify decomposition calculation

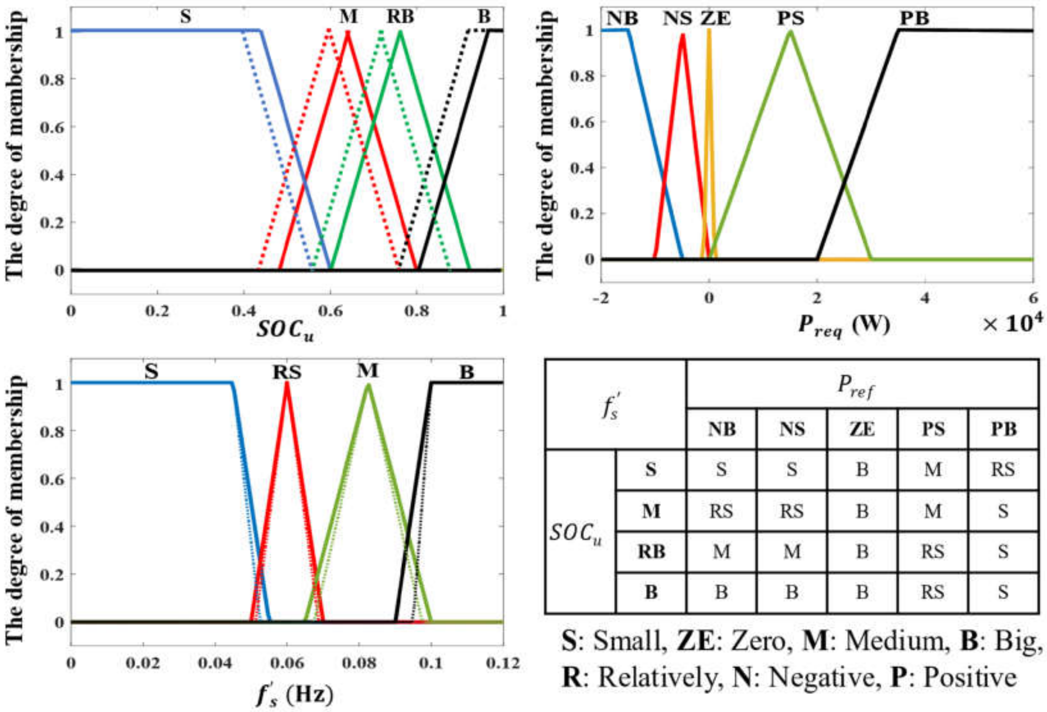

f_s'		P_{ref}				
		NB	NS	ZE	PS	PB
SOC_u	S	S	S	B	M	RS
	M	RS	RS	B	M	S
	RB	M	M	B	RS	S
	B	B	B	B	RS	S

Fig. 6: FC#1 rule base and membership functions

complexity. The mother Haar wavelet function can be expressed as follows:

$$\Psi_{Haar}(t)=\begin{cases}+1 & 0\le t\le 0.5\\ -1 & 0.5<t\le 1\\ 0 & otherwise\end{cases} \quad (13)$$

As indicated in Fig. 7, a three-level Haar wavelet transforms, as an optimal transform method, is utilized to perform on the original signal $s(n)$. Hence, a low-pass filter $l_0(z)$ decomposes the original signal $s(n)$ into the fundamental signal, and the defined wavelet transform reconstructs it into the original signal with low errors based on the low and high-pass filters on the reconstruction side. Therefore, the signal processing unit separates the low and high-frequency components of P_{fc-b} directly.

Based on simulation results, the error of the reconstruction process is less than 10^{-10}. Hence, the defined wavelet method is extremely reliable, and the EMS of FCHEV employs it as a simple and real-time signal processing state.

Although the three-level decomposition is selected as the optimal level, there are notable differences among the required power and decomposition levels. According to [25] and [26], the effective method, as an expression between the signal frequency and the decomposition level, is determined and summarized as follows:

$$n=\left\lfloor\frac{\log(f_{sample}/f_c)}{\log(2)}-1\right\rfloor \quad (14)$$

where f_{sample} and f_c are defined as the sampling frequency and the frequency of power demand on the battery pack based on the n-level decomposition, respectively. Consequently, the frequency of power demand on the battery system was obtained as $[10^{-2},10^{2}]$ Hz range. Also, the sampling frequency of the power demand is calculated at 1Hz. Therefore, the defined wavelet method utilizes such 10^{-2}, 10^{-1}, 10^{0}, 10^{1}, and 10^{2}Hz as representative decomposition frequencies. Furthermore, the optimal decomposition level has a range of [2, 5] while $n = 3$is selected as the optimal decomposition level.

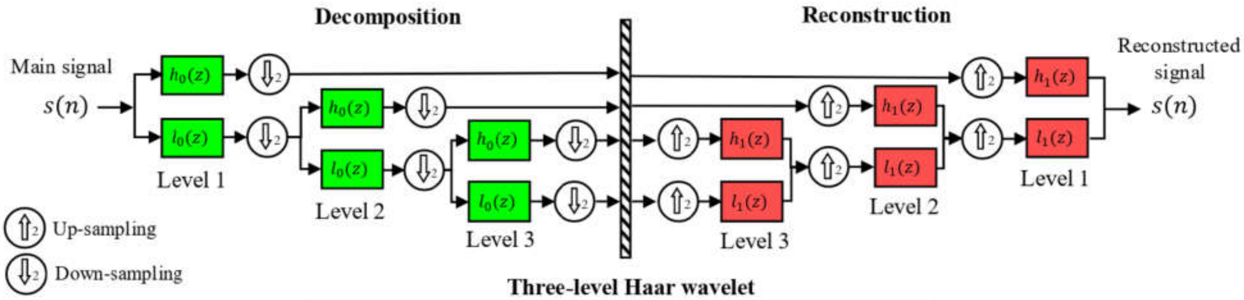

Fig. 7: Three-level Haar wavelet transform process schematic

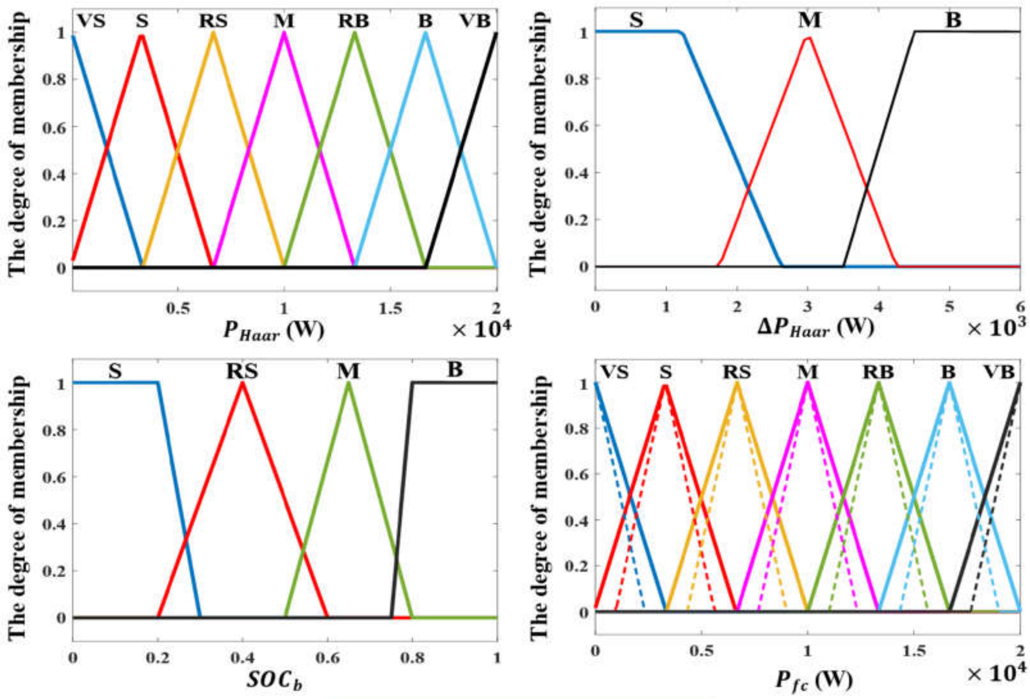

Fig. 8: Membership functions of FC#2

Table 3: FC#2 rule bases

P_{fc}		P_{Haar} (ΔP_{Haar}= S, M, B)						
		VB	**B**	**RB**	**M**	**RS**	**S**	**VS**
SOC_b	**S**	VB, VB, VB	VB, VB, VB	VB, VB, VB	B, B, B	RB, RB, RB	M, M, M	RS, RS, RS
	RS	VB, VB, VB	VB, VB, VB	B, B, B	RB, RB, RB	M, M, M	RS, RS, RS	S, S, S
	M	VB, B, B	B, RB, RB	RB, M, M	M, RS, RS	RS, S, S	S, S, VS	VS, VS, VS
	RB	B, RB, RB	RB, M, M	M, RS, RS	RS, S, S	S, S, VS	VS, VS, VS	VS, VS, VS

3.3. Power Sharing Algorithm Based on Type-II Fuzzy Control

The wavelet transform provides a main approximation of the fuel cell power as a reference power signal. Furthermore, the battery beside the ultra-capacitor system should have enough charge level to supply/absorb the FCHEV power in acceleration/braking states and to modify a tolerable range for the battery and ultra-capacitor SOC.

For high-efficiency performance, the fuel cell system should supply power in the high-efficiency region as shown in Fig. 2. Therefore, the fuel cell can stabilize the energy distribution system against overcharging and over-discharging of the battery. Consequently, the type-II fuzzy control (FC#2) is designed to calculate optimal fuel cell power to satisfy improving the durability and fuel economy of the fuel cell system as primary advantages.

The fuel cell reference power (P_{Haar}), differential of fuel cell reference power (ΔP_{Haar}), and battery SOC (SOC_b) apply to FC#2 as input variables, and the fuel cell power P_{fc} considers the output variable. For FC#2, the membership function and fuzzy rule bases are illustrated in Fig. 8 and Table 3 respectively.

According to the rule bases of FC#2, the fuel cell system will supply high-level power when the battery SOC is small. When SOC_b is small or rather small, to maintain battery SOC in the high-level charge, P_{fc}^{ref} should determine the big state and vice versa. FC#2's major objective is a reduction in fuel consumption (an improvement on fuel economy) by using the battery system's efficiency, whenever SOC_b should have a suitable charge level, and by maintaining it within a tolerable range. The sharp fluctuation on fuel cell reference power is one of the main challenges of EMSs to improve the durability and efficiency performance of a fuel cell system. The sharp signal required power sets the fuel cell system in a sudden power generation situation; therefore, the durability will be reduced after a long operation of the fuel cell system. As a solution to prevent a sharp signal effect on the fuel cell power, the differential signal of reference fuel cell power (ΔP_{Haar}) is defined to increase the fuel cell power step by step.

4. Simulation and Verification Results

For verification, the proposed EMS was compared to similar works by using MATLAB/SIMULINK and ADVISER simulator. Therefore, the power transmission parameters are reported in Table 4 for the simulated FCHEV in MATLAB/SIMULINK environment.

In the first, the initial value of SOC_b and SOC_u were assumed 0.7 and 0.8 respectively. As known, the EMS of FCHEV has a direct effect on the maximum output power. As a result, the fuel cell system's dynamically delayed operation prevents the vehicle from instantaneously attaining its full output power. Meanwhile, the SOC of the battery and ultra-capacitor was modified by the proposed EMS in order to prevent overcharge and over-discharge states, which had considerable efficiency in the dynamic performance.

This study utilized a valid driving cycle database to evaluate the proposed EMS on a typical road and driving conditions. As illustrated in Fig. 9(a), the test database was a combination of the three driving cycles such as the Dynamometer Driving Schedule (UDDS), Highway Fuel Economy Test (HWFET), and Extra Urban Driving Cycle (EUDC&ECE), which represent city, highway, and suburban respectively [27]. Hence, the compound driving cycle can be represented as follows:

- The UDDC cycle refers to the United States Environmental Protection Agency-mandated dynamometer test on fuel economy; it represents urban driving conditions that are used for light-duty vehicle testing.
- The HWFET cycle represents highway driving conditions under 60 mph.
- The EUDC cycle has been designed to represent more aggressive, high-speed driving modes, and the ECE cycle has been devised to represent city driving conditions, e.g., in Paris or Rome.

Hence, the proposed EMS was analyzed under selected driving cycles' database as the vehicle speed profiles. Consequently, the vehicle speed profiles and the required power are indicated in Fig. 9(a) and Fig. 9(b) respectively. Furthermore, simulation results were shown in Figures 10 and 11.

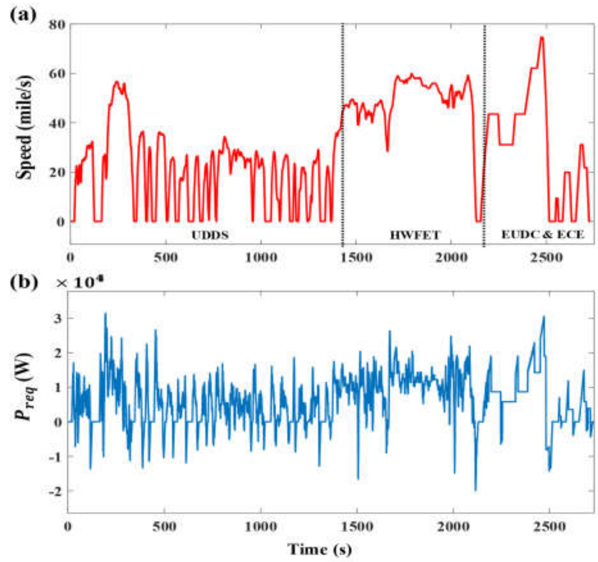

Fig. 9: (a) The vehicle speed profile based on triple driving cycles, (b) The required power of FCHEV

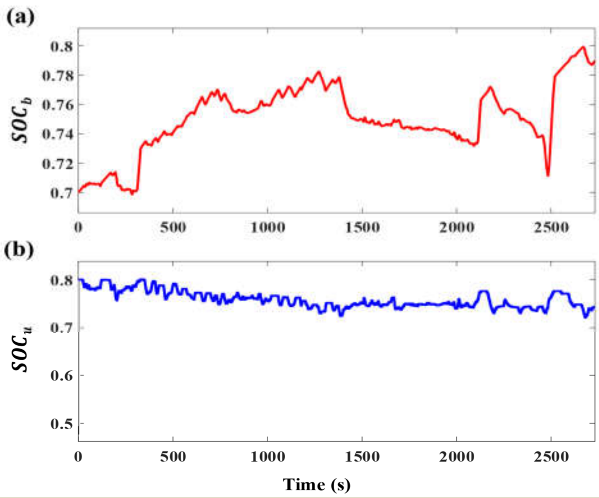

Fig. 10: Simulation results of (a) battery, and (b) ultracapacitor SOC

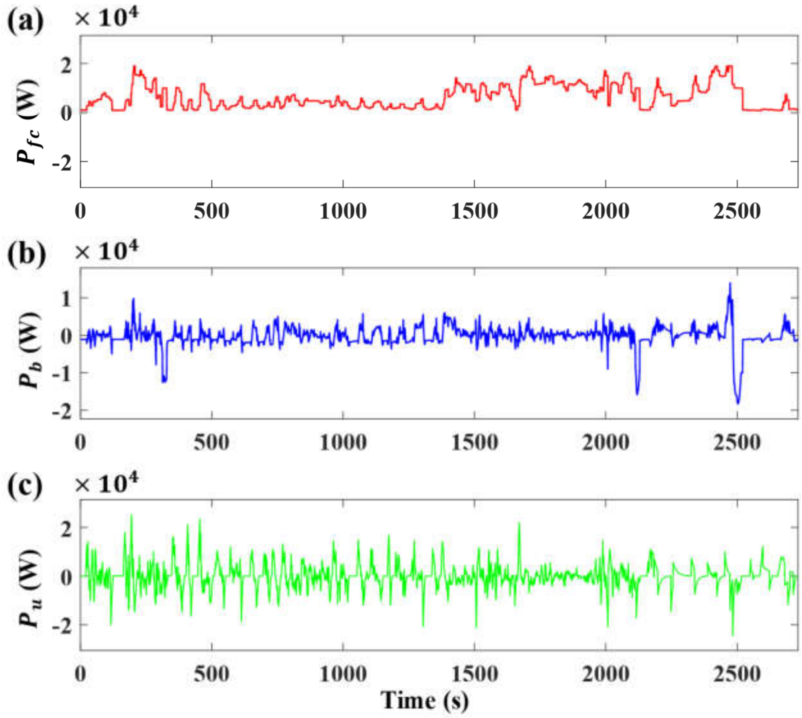

Fig. 11. The simulation results of EMS proposed in triple driving cycles: Optimal distributed power of (a) fuel cell, (b) battery, and (c) ultracapacitor units

4.1. Optimal Power Distribution

As stated earlier, Fig. 9(b) and Fig. 11show the simulation results of the required power and optimal distributed power respectively. As shown, the battery and ultra-capacitor systems play a major role to supply the required power during the UDDC cycle. Because the required power in this driving cycle contains extremely high acceleration and braking states. To avoid high-frequency power distribution on the fuel cell system, the battery and ultra-capacitor systems deliver the majority of the required power. In the other conditions, the HWFET and EUDC&ECE driving cycles have requested enormous power values with a lower frequency component securely. As a result, the fuel cell system, as the primary power supply, provides the majority of the required power.

The ultra-capacitor system can supply the instant growth of the required power in an acceleration state (as shown in Fig. 11(c)). Therefore, the proposed EMS decreases power fluctuations on the fuel cell system to improve the durability and reactivity (as shown in Fig. 11(a)). As illustrated in Fig. 11(b), the battery system supplies stable power to reduce fluctuations in fuel cell power. Furthermore, the fuel cell system always generates power with a 2.5kW minimum limit (high-efficiency region of fuel cell operation in Fig. 2) to satisfy the battery charge state stabilization approach, which can improve fuel economy by reducing hydrogen consumption.

Table 4: The power transmission system parameters [28]

Systems	Type	Parameters
Motor	PMSM	Max torque (N.m): 488 Max power (kW): 75 Average efficiency (%): 90
Fuel cell	PEM	Total mass (kg): 163 Max net power (kW): 30 Average efficiency (%): 56
Battery	Li-ion	Max capacity (kWh): 9.25 Max power (kW): 20 Average efficiency (%): 85
Ultracapacitor	Maxwell	Max capacity (Wh): 350 Max power (kW): 70 Average efficiency (%): 98
DC-DC converter	-	Max efficiency (%): 90

The simulation result in Fig. 10 indicates the battery and ultra-capacitor SOCs separately. In order to maintain the battery SOC in the tolerable range, the proposed EMS distributes the required power on the battery system by less than 5% fluctuation, which can make FCHEV maintain the battery and ultra-capacitor SOCs on the tolerable range, and FCHEV would be able to drive more distances in hydrogen limitation case.

4.2. Power Transient Response Analysis

A power transient response is the response of a power system to a change from the steady state. It is not necessarily tied to unwanted events, but to any event that affects the steady state of the system.

Therefore, the fuel cell output power transient response as a fluctuation metric [21] is a valid criterion that can effectively improve the fuel cell durability. Hence, simulation results reported fuel cell power fluctuation in the -200W/s to +200W/s range. Furthermore, based on the same driving cycle, the presented EMS in [29] and [30] obtained the fuel cell power fluctuations in the ±1000W/s and ±500W/s ranges respectively (as shown in Fig. 12). According to this valid comparison, the differential of fuel cell reference power (ΔP_{Haar}) as an input variable of FC#2 played an effective role to modify power fluctuations in order to improve the durability of the fuel cell system.

4.3. Hydrogen Consumption

In this study, fuel economy improvement was concentrated as a primary purpose. Therefore, it was an extremely notable advantage to guarantee that the proposed EMS had a valid trade-off between defined optimization objections.

For a valid comparison, the equivalent hydrogen consumption was defined as a function of the fuel cell power, the battery SOC, and the ultra-capacitor SOC.

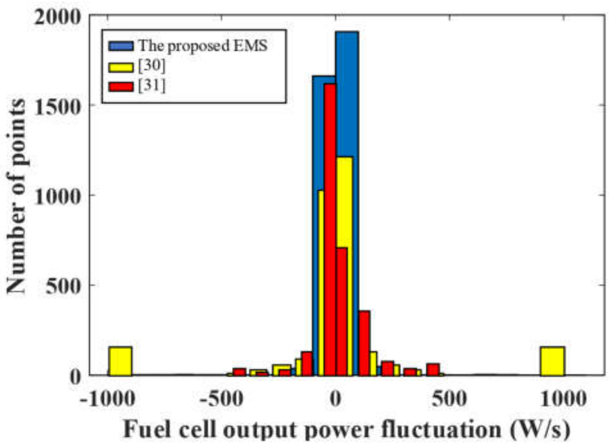

Fig. 12: Comparison of fuel cell power fluctuation between different EMSs

Hence, the equivalent hydrogen consumption is determined as follows:

$$C_{H_2} = \int_0^t \frac{P_{fc}(t)}{\eta_{fc}\rho_{H_2}} dt + \frac{\Delta SOC_b \cdot f_b \cdot 3600}{\eta_{fc}\rho_{H_2}} + \frac{\Delta SOC_u \cdot f_u \cdot 3600}{\eta_{fc}\rho_{H_2}} \quad (15)$$

where C_{H_2} is defined as equivalent hydrogen consumption for the proposed FCHEV. The hydrogen chemical energy density ρ_{H_2} is related to equivalent factors of battery f_b and ultra-capacitor f_u. Also, ΔSOC_b and ΔSOC_u are the difference value between the final and initial battery and ultra-capacitor SOCs.

According to Eq. (14) and the simulation results for the compound driving cycle, the hydrogen consumption of the proposed EMS was calculated at 15.56 liters. Hence, the proposed EMS saved about 8.8% and 14.6% of hydrogen in comparison to [30] and [29] under the same driving cycle respectively. In addition, Fu et al. [19] presented two different parametric fuzzy control based on a genetic algorithm under different driving cycles. Therefore, the hydrogen consumption values are reported as 17.159 and 17.667 liters based on two different strategies. For an equitable evaluation, the proposed EMS is simulated under the same driving cycle in [31]. Thus, the proposed EMS could present a 9.5% reduction in hydrogen consumption to improve the efficiency performance of the fuel cell system in FCHEV.

4.4. Method Verification with ADVISOR Simulator

ADVISOR simulator implements control strategies for hybrid electric vehicles based on MATLAB/SIMULINK by various subsystems. Furthermore, ADVISOR utilizes different related technology such as the fuel cell, battery, ultra-capacitor, and hybrid electric vehicle propulsion systems to determine the fuel consumption, pollutant emission, and dynamic efficiency of the electric vehicle [32]. In order to verify the proposed EMS, the researchers could replace their own innovative methods as EMS unit in ADVISOR and examined their proposed method using the different valid tests to check the vehicle's performance in driving conditions, hill climbing, and acceleration.

According to system parameters in Table 5, the dynamic performance test was simulated for the proposed EMS by the ADVISOR simulator. Therefore, Table 6 reported the dynamic performance test of FCHEV based on the proposed EMS by the ADVISOR simulator. In similar driving conditions, the proposed EMS improved the vehicle acceleration time for 0-100km/h by 32.8% and 12.65% than the presented EMSs in [29] and [30] respectively. In addition, other acceleration parameters reported considerable improvement than other EMS based on different fuzzy control approaches.

Table 5: The system parameters of FCHEV in ADVISOR simulator [29 & 30]

Parameters	Value
Fuel cell rate power (kW)	10
Output voltage range of fuel cell (V)	40-100
Unidirectional DC/DC converter rate power (kW)	10
Battery energy (kWh)	25.6
Ultra-capacitor energy (Wh)	320
Output voltage range of ultracapacitor (V)	128-288
Bidirectional DC/DC converter rate power (kW)	10
Motor rate power (kW)	45

Table 6: The results of comparison of vehicle dynamic performance test using ADVISOR simulator

Parameters	The proposed EMS	[29]	[30]
Acceleration time for 0-100 km/h (s)	8.21	13.3	9.4
Acceleration time for 64-97 km/h (s)	4.86	6.9	5.2
Acceleration time for 0-137 km/h (s)	22.14	31.1	26.7
Maximum acceleration rate (m/s^2)	5.02	4.94	4.94
Maximum speed (km/h)	154.12	150	150

5. Conclusion

In this paper, a novel EMS based on the type-II fuzzy control, adaptive low-pass filter, and Haar wavelet transform has been proposed for the fuel cell/battery/ultra-capacitor hybrid electric vehicle. Furthermore, improving durability and fuel economy in fuel cell systems, as research issues, have been investigated under valid driving conditions.

The uncertainty on the charge state of battery and ultra-capacitor systems made a sufficient motivation to utilize type-II fuzzy controllers as a simple and real-time control method. Therefore, the proposed EMS decomposes the vehicle's required power into different frequency components based on uncertainty over the output of the type-II fuzzy controllers. The adaptive low-pass filter filtered the high-frequency component of the required power signal; then, the Haar wavelet transform applied a pre-processing to obtain a smooth reference power signal as basic fuel cell power.

A significant benefit of increasing the lifespan of systems under the compound driving cycle has been provided by the modeling of the proposed EMS mentioned throughout multiple distinct analyses, which showed fuel cell and battery systems ensured that transition changes never occured through the required power. In contrast to existing EMSs, the suggested EMS was able to sustain a considerable amount of hydrogen, which demonstrated higher fuel economy performance. The ADVISOR simulator evaluates the dynamic performance test of the FCHEV, which led into acceptable results when compared to other EMSs over the same driving cycle.

Nomenclature

FCHEV	Hybrid electric vehicle with fuel cell/battery/ultracapacitor	R_c	Equivalent resistance (Ω)
		i_c	Capacitor current (A)
EMS	Energy management strategy	SOC_u	Ultracapacitor SOC
SOC	State of charge	$V_{uc,max}$	Ultracapacitor maximum voltage (V)
v	Vehicle speed (m/s)	P_{fc-b}	Fuel cell and battery power (W)
F_t	Traction force (N)	P_{Haar}	Fuel cell reference power (W)
F_f	Friction resistance with road surface (N)	ΔP_{Haar}	Differential of fuel cell reference power
F_w	Aerodynamic drag force (N)	T	Time constant of the low-pass filter (s)
F_i	Gravity force (N)	f_s	Regulating frequency (Hz)
F_j	Vehicle accelerate force (N)	FC	Fuzzy controller
f_r	Rolling resistance coefficient	SOC_u^{ref}	Ultracapacitor reference SOC
m	Vehicle mass (kg)	f_s'	Final corrected regulating frequency (Hz)
g	Gravity constant (m/s^2)	Δf_s	Adjusting frequency increment (Hz)
α	Road angle (Rad)	k	Regulatory factor
C_d	Aerodynamic drag coefficient	s	Original signal
A	Vehicle frontal area (m^2)	λ	Scale parameter
ρ	Air density (kg/m^3)	u	Position parameter
δ	Conversion coefficient of vehicle rotating mass	W	Wavelet coefficient
		f_{sample}	The battery sampling frequency (Hz)
P_{req}	Required power of the vehicle (W)	f_c	The frequency of power demand on the battery (Hz)
η_m	Efficiency of the electric motor (%)		
η_{fc}	Global efficiency of fuel cell system (%)	n	Wavelet decomposition level
P_{fc}	Fuel cell power (W)	UDDS	Dynamometer Driving Schedule
P_{H_2}	Theoretical power (W)	HWFET	Highway Fuel Economy Test
V_b	Battery output voltage (V)	EUDC&ECE	Extra Urban Driving Cycle
E_b	Battery open voltage (V)	C_{H_2}	Equivalent hydrogen consumption of FCHEV (Liter)
R_b	Internal resistance (Ω)		

i_b	Battery current (A)	ρ_{H_2}	Hydrogen energy density $(\mathrm{M}J/kg)$
SOC_b	Battery SOC	f_b	Equivalent factors of battery
$SOC(1)$	Initial battery SOC	f_u	Equivalent factors of ultracapacitor
η_b	Battery charge/discharge efficiency (%)	ΔSOC_b	Indexed value of the difference between final and initial SOC_b
Q_b	Battery nominal capacity (kWh)		
V_u	Ultracapacitor terminal voltage (V)	ΔSOC_u	Indexed value of the difference between final and initial SOC_u
E_u	Capacitor voltage (V)		

References

[1] Sun, Z., Wang, Y., Chen, Z. and Li, X., "*Min-max game-based energy management strategy for fuel cell/supercapacitor hybrid electric vehicles*", Applied energy, Vol. 267, pp. 115086, 2020, doi:10.1016/j.apenergy.2020.115086.

[2] Kang, J., Guo, Y. and Liu, J., "*Rule-based energy management strategies for a fuel cell-battery hybrid locomotive*", In 2020 IEEE 4th Conference on Energy Internet and Energy System Integration (EI2), pp. 45-50, 2020, doi:10.1109/EI250167.2020.9346652.

[3] Bianchi, D., Rolando, L., Serrao, L., Onori, S., Rizzoni, G., Al-Khayat, and et al., "*January. A rule-based strategy for a series/parallel hybrid electric vehicle: an approach based on dynamic programming*", In Dynamic Systems and Control Conference, Vol. 44175, pp. 507-514, 2010, doi:10.1115/DSCC2010-4233

[4] Chen, S.Y., Wu, C.H., Hung, Y.H. and Chung, C.T., "*Optimal strategies of energy management integrated with transmission control for a hybrid electric vehicle using dynamic particle swarm optimization*", Energy, Vol. 160, pp. 154-170, 201, doi:10.1016/j.energy.2018. 06.023.

[5] Fathy, A., Rezk, H. and Nassef, A.M., "*Robust hydrogen-consumption-minimization strategy based salp swarm algorithm for energy management of fuel cell/supercapacitor/batteries in highly fluctuated load condition*", Renewable energy, Vol. 139, pp. 147-160, 2019, doi:10.1016/j.renene.2019.02.076.

[6] Li, X., Wang, Y., Yang, D. and Chen, Z., "*Adaptive energy management strategy for fuel cell/battery hybrid vehicles using Pontryagin's Minimal Principle*", Journal of Power Sources, Vol. 440, pp. 227105, 2019, doi:10.1016/j.jpowsour.2019.227105.

[7] Huo, X., Ma, L., Zhao, X., Niu, B. and Zong, G., "*Observer-based adaptive fuzzy tracking control of MIMO switched nonlinear systems preceded by unknown backlash-like hysteresis*", Information Sciences, Vol. 490, pp.369-386, 2019, doi:10.1016/j.ins.2019.03. 082.

[8] Chen, J., Xu, C., Wu, C. and Xu, W., "*Adaptive fuzzy logic control of fuel-cell-battery hybrid systems for electric vehicles*", IEEE transactions on industrial informatics, Vol. 14, pp. 292-300, 2016, doi:10.1109/TII.2016.2618886.

[9] Hagras, H., "*Type-2 FLCs: A new generation of fuzzy controllers*", IEEE Computational Intelligence Magazine, Vol. 2, pp. 30-43, 2007, doi:10.1109/MCI.2007.357192.

[10] C. Jia, J. Cui, W. Qiao, and L. Qu, "*A Real-time Operational Cost Minimization Strategy for Energy Management of Fuel Cell Electric Vehicles*", 2021 IEEE Energy Conversion Congress and Exposition (ECCE), 2021, doi:10.1109/ECCE47101.2021.9595701.

[11] D. Li, B. Xu, J. Tian, and Z. Ma, "*Energy Management Strategy for Fuel Cell and Battery Hybrid Vehicle Based on Fuzzy Logic*", Processes, Vol. 8, No. 8, pp. 882, 2020, doi:10.3390/pr8080882.

[12] Y. Liu, J. Liang, J. Song and J. Ye, "*Research on Energy Management Strategy of Fuel Cell Vehicle Based on Multi-Dimensional Dynamic Programming*", Automot. Eng, Vol. 41, pp.1347-1355, 2019, doi: 10.3390/ en15145190.

[13] G. Zhang, W. Chen, and Q. Li, "*Modeling, optimization and control of a FC/battery hybrid locomotive based on ADVISOR*", International Journal of Hydrogen Energy, Vol. 42, No. 29, pp. 18568–18583, 2017, doi:10.1016/j.ijhydene.2017.04.172.

[14] X. Lü et al., "*Energy management of hybrid electric vehicles: A review of energy optimization of fuel cell hybrid power system based on genetic algorithm*", Energy Conversion and Management, Vol. 205, pp. 112474, 2020, doi:10.1016/j.enconman.2020.112474.

[15] C. Wang, R. Liu, and A. Tang, "Energy management strategy of hybrid energy storage system for electric vehicles based on genetic algorithm optimization and temperature effect", Journal of Energy Storage, Vol. 51, pp. 104314, 2022, doi:10.1016/j.est .2022.104314.

[16] D. Min, Z. Song, H. Chen, T. Wang, and T. Zhang, "*Genetic algorithm optimized neural network-based fuel cell hybrid electric vehicle energy management strategy under start-stop condition*", Applied Energy, Vol. 306, pp. 118036, 2022, doi:10.1016/j.apenergy .2021.118036.

[17] Bourdim, S., Azib, T., Hemsas, K.E. and Larouci, C., "*Efficient energy management strategy for fuel cell ultracapacitor hybrid system*", In 2016 Int. Conf. on Elec. Sys. for Air., Rail., Ship Prop. and Road Veh.& Int. Tran. Elec. Conf. (ESARS-ITEC), pp. 1-6, 2016, doi:10.1109/ESARS-ITEC.2016.7841325.

[18] Singh, K.V., Bansal, H.O. and Singh, D., "*Fuzzy logic and Elman neural network tuned energy management strategies for a power-split HEVs*", Energy, Vol. 225, pp. 120152, 2021, doi:10.1016/j.energy.2021. 120152.

[19] García, P., Fernández, L.M., Torreglosa, J.P. and Jurado, F., "*Operation mode control of a hybrid power system based on fuel cell/battery/ultracapacitor for an electric tramway*", Computers & Electrical Engineering, Vol. 39, pp. 1993-2004, 2013, doi:10.1016/j. compeleceng.2013.04.022.

[20] Zhou, D., Al-Durra, A., Gao, F., Ravey, A., Matraji, I. and Simoes, M.G., "*Online energy management strategy of fuel cell hybrid electric vehicles based on data fusion approach*", Journal of power sources, Vol.366, pp.278-291, 2017, doi:10.1016/j.jpowsour.2017.08. 107.

[21] Zhang, R., Tao, J. and Zhou, H., "*Fuzzy optimal energy management for fuel cell and supercapacitor systems using neural network-based driving pattern recognition*", IEEE Transactions on Fuzzy Systems, Vol. 27, pp. 45-57, 2018, doi:10.1109/TFUZZ.2018.2856086.

[22] Liang, Q., Karnik, N.N. and Mendel, J.M., "*Connection admission control in ATM networks using survey-based type-2 fuzzy logic systems*", IEEE Transactions on Systems, Man, and Cybernetics, Part C (Applications and Reviews), Vol. 30, pp. 329-339, 2000, https://doi.org /10.1109/5326.885114.

[23] Mattavelli, P., Rossetto, L., Spiazzi, G. and Tenti, P., "*General-purpose fuzzy controller for DC-DC converters*", IEEE transactions on Power Electronics, Vol. 12, pp. 79-86, 1997, doi:10.1109/63.554172.

[24] Wang, C., Xiong, R., He, H., Zhang, Y. and Shen, W., "*Comparison of decomposition levels for wavelet transform based energy management in a plug-in hybrid electric vehicle*", Journal of cleaner production, Vol. 210, pp. 1085-1097, 2019, doi:10.1016/j.jclepro .2018.11.082.

[25] Ibrahim, M., Jemei, S., Wimmer, G. and Hissel, D., "*Nonlinear autoregressive neural network in an energy management strategy for battery/ultra-capacitor hybrid electrical vehicles*", Electric Power Systems Research, Vol. 136, pp. 262-269, 2016, doi:10.1016/j.epsr.2016.03.005.

[26] Ibrahim, M., Jemei, S., Wimmer, G., Steiner, N.Y., Kokonendji, C.C. and Hissel, D., "*Selection of mother wavelet and decomposition level for energy management in electrical vehicles including a fuel cell*", International journal of hydrogen energy, Vol. 40, pp. 15823-15833, 2015, doi:10.1016/j.ijhydene.2015.06.055.

[27] US EPA, OAR, "*Dynamometer Drive Schedules | US EPA*", US EPA, Sep. 16, 2015, https://www.epa.gov/vehicle-and-fuel-emissionstesting /dynamometer-drive-schedules.

[28] Z. Fu, Z. Li, P. Si, and F. Tao, "*A hierarchical energy management strategy for fuel cell/battery/supercapacitor hybrid electric vehicles*", International Journal of Hydrogen Energy, Vol. 44, No. 39, pp. 22146–22159,2019, doi:10.1016/j.ijhydene.2019.06. 158.

[29] Zhang, Q. and Li, G., "*A predictive energy management system for hybrid energy storage systems in electric vehicles*", Electrical Engineering, Vol. 101, pp. 759-770, 2019, doi:10.1007/s00202-019-00822-9.

[30] Hemi, H., Ghouili, J. and Cheriti, A., "*A real time fuzzy logic power management strategy for a fuel cell vehicle*", Energy conversion and Management, Vol. 80, pp. 63-70, 2014, doi:10.1016/j.enconman.2013.12.040.

[31] Fu, Z., Zhu, L., Tao, F., Si, P. and Sun, L., "*Optimization based energy management strategy for fuel cell/battery/ultracapacitor hybrid vehicle considering fuel economy and fuel cell lifespan*", International Journal of Hydrogen Energy, Vol. 45, pp. 8875-8886, 2020, doi:10.1016/j.ijhydene.2020.01.017.

[32] Adv-vehicle-sim.sourceforge.net. (n.d.). "*ADVISOR Documentation*", 2023, Available at: https://adv-vehicle-sim.sourceforge.net.